LASER INTERFEROMETER GRAVITATIONAL WAVE OBSERVATORY
- LIGO -
CALIFORNIA INSTITUTE OF TECHNOLOGY
MASSACHUSETTS INSTITUTE OF TECHNOLOGY

Technical Note	**LIGO-T11XXXXX–vX**	2014/09/26

Implementing A Frequency Control Loop for the 40m Prototype Arm Length Stabilization System

SURF Students: Andrew Hall Mentors: Manasadevi P Thirugnanasambandam, Eric Quintero, Koji Arai

California Institute of Technology
LIGO Project, MS 18-34
Pasadena, CA 91125
Phone (626) 395-2129
Fax (626) 304-9834
E-mail: info@ligo.caltech.edu

Massachusetts Institute of Technology
LIGO Project, Room NW22-295
Cambridge, MA 02139
Phone (617) 253-4824
Fax (617) 253-7014
E-mail: info@ligo.mit.edu

LIGO Hanford Observatory
Route 10, Mile Marker 2
Richland, WA 99352
Phone (509) 372-8106
Fax (509) 372-8137
E-mail: info@ligo.caltech.edu

LIGO Livingston Observatory
19100 LIGO Lane
Livingston, LA 70754
Phone (225) 686-3100
Fax (225) 686-7189
E-mail: info@ligo.caltech.edu

http://www.ligo.caltech.edu/

1 Introduction: The LIGO Detector

Gravitational waves are a component of Einstein's theory of General Relativity, which have not, as of yet, been directly observed. The detection, observation and characterization of these waves are the primary goals of the LIGO detector.

The waves manifest themselves with disturbances in spacetime, causing miniscule changes in length. These modulations, when detected, are on the scale of $10^{-18}m$ [1]. With independent variables on such a small scale, it is necessary to employ a highly sensitive instrument–in this case, a laser interferometer, diagrammed in Figure 1.

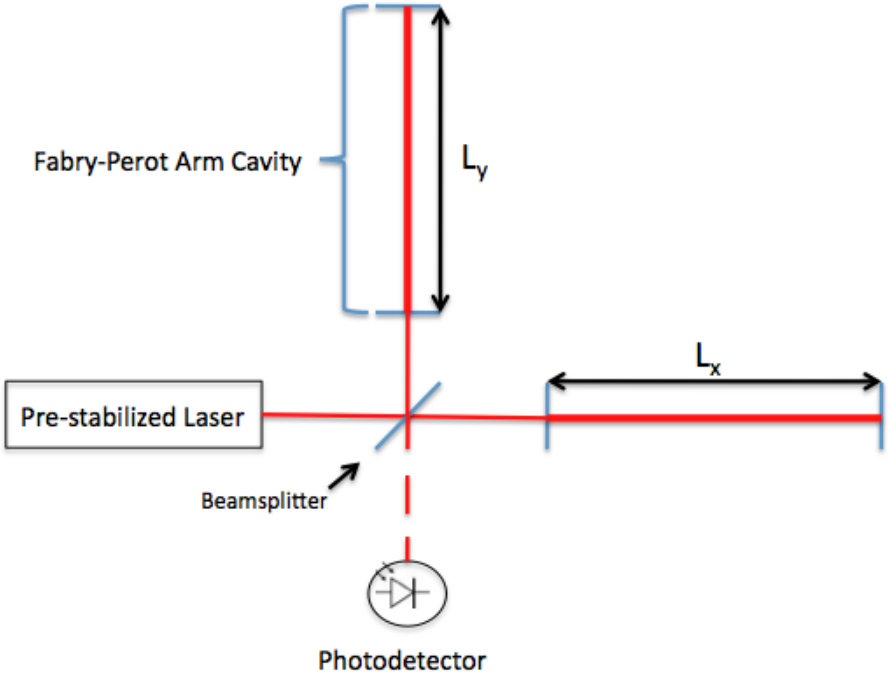

Figure 1: Laser interferometer with Fabry-Perot arm cavities.

Since the laser light is perfectly in phase with itself when it enters the arm-cavities, the only thing that could shift the phase difference between beams is a difference in arm length $(L_x - L_y)$. Thus, we can observe changes on the scale in which we need to. Measurements are taken by way of observing interference patterns produced by the recombined beam.

The Fabry-Perot arm-cavities, as opposed to the more traditional simple arms, allow us to generate greater arm lengths, and thus increase sensitivity, which increases in proportion to arm length.

In addition to the Fabry-Perot arm cavities, the detector implements power recycling cavities at the vertex of the detector, which effectively amplify the optical power of the PSL, improving the shot noise level [3]

2 Arm Length Stabilization (ALS)

In order to operate such a sensitive interferometer, we must know and control the degrees of freedom of the Fabry-Perot arm cavities. In order to do so, we make use of a frequency doubled auxiliary laser (AUX) system, which operates at baseline 536 nm. The AUX frequency can vary, as it is locked to the arm cavity length by a Pound-Driver-Hall locking servo. Using this frequency as the measurement of the arm cavity length, it is then possible to bring the PSL into lock with AUX, and thereby, the arm cavity length. The length detection scheme is described below, v and δv referring to the baseline frequency, and change in frequency, and L and δL referring to the baseline length, and change in length.

$$\frac{\delta v_a(t)}{\overline{v}} = -\frac{\delta L(t)}{\overline{L}} \text{ [2]}$$

In this system, an AUX beam is injected through the Fabry-Perot arm cavity, then combined with the frequency doubled prestabilized laser (PSL) to beat with each other, and is fed into a photodiode which acts as an input to a delay-line frequency discriminator (DFD). The DFD functions to create a linear error signal, which is then used to correct the arm cavity length through servo controlled end test masses (ETM) [2].

3 Problem

The problem here lies within the offsetting system used to keep the AUX laser locked with the arm cavity length. The laser cavity actuators can only respond at $5\frac{MHz}{V}$ with a range of $\pm 10V$, while the arm cavity length can fluctuate on a length scale corresponding to a frequency range well beyond that of the laser cavity actuators [2]. It is clear that we are in need of another method of control, with a greater range.

When we sense a beat frequency >100MHz, we encounter difficulty, since we are outside the ALS system's effective working range. This is where the proposed new servo comes into play. Using a separate sample of each beam, (AUX and PSL) we will use their beat frequency to generate a digital error signal, which will be fed into a digital PID loop, and used to actuate the temperature control of AUX, in order to bring it back into within the working range of the ALS system.

We implement a temperature actuator, which will control the temperature of the crystal within the laser, yielding a controllable range of roughly $1\frac{GHz}{V}$. This servo will respond to signals below about 1 Hz.

4 Preliminary Design and Working Principles

In principle, the temperature actuator will modulate the temperature of the laser crystal when there is a signal of frequency below 1 Hz. Changing the temperature of the crystal changes its physical dimensions, and thereby modulates its frequency in proportion.

We will take beam samples of the AUX and PSL, and recombine them at the vertex of the detector. The combined beam will then enter a photodiode. This signal will enter a frequency counter, which will then give a remote readout of the beat frequency, and then go on to the digital PID loop, which will eventually go through the DAC to actuate the temperature control servo, and bring the AUX frequency back within a workable range.

This design is show in Figure 2.

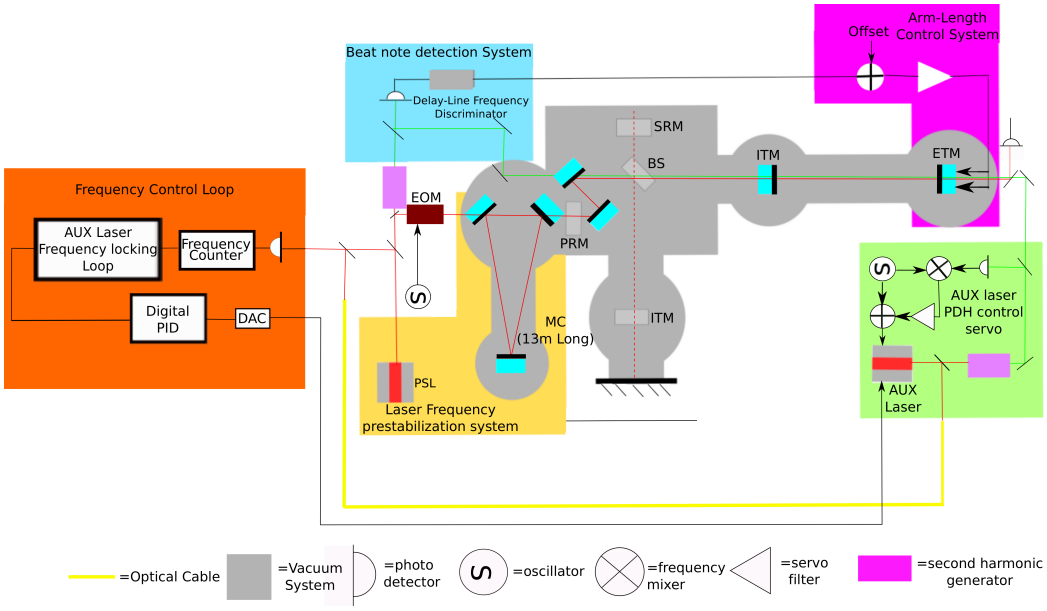

Figure 2: Schematic of interferometer with proposed AUX laser frequency locking loop

5 Current Progress

My part of the Frequency Offset Locking setup is essentially comprised of the optics that will sample the AUX and PSL beams, and combine them to produce the beat note error signal. In order to do this, we will be coupling NPRO light into Polarization Maintaining (PM) fibers (Corning PANDA PM980). Coupling, i.e. mode matching, requires knowledge of the laser modes. In order to characterize the laser modes, we need to measure the size and location of the beam waists, as the rest of the beam can be extrapolated from these data, given that the laser propagates as a Gaussian beam. Thus, the first order of business was to characterize the waists of the sample light from both PSL and AUX lasers.

Once these data were taken, I continued to design a telescope, with which I will couple laser light into the fibers, for further use in the frequency offset locking (FOL) setup.

6 Methods of Waist Measurement

In order to measure the beam waist, I have been using the "Knife-Blade" measurement technique. This technique involves shining the laser (spare 1064nm NPRO) on a photodiode. The razor blade setup is pictured below in Figure 3

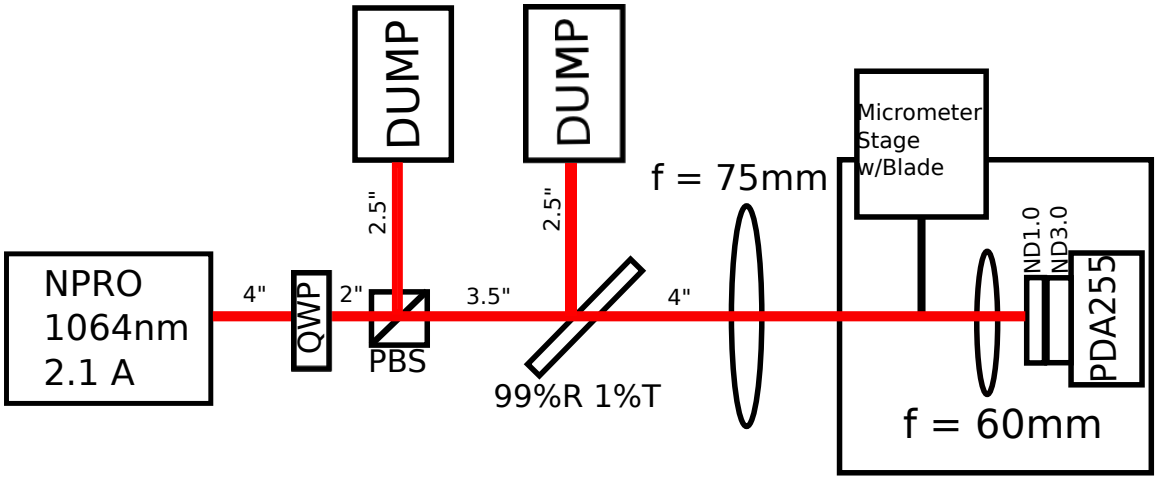

Figure 3: The razor blade setup used

Note: PBS stands for "Polarizing Beam Splitter" and 99%R 1%T is a 99% Reflective, 1% Transmissive mirror.

A razor blade is then translated orthogonally (both in the X and Y directions) to the beam via a micrometer stage, and measurements of the power on the photodiode are taken periodically in order to generate data that describe the fraction of total optical power contained in a given fraction of the beam's cross section at a specific point along the direction of propagation. These data are taken at multiple points along the optical axis. They are then fit to the following equation:

$$V_{measured} = \frac{V_{max}}{2}[1 \pm erf(\frac{\sqrt{2}(x-x_o)}{w_o})]$$

[5]

Where $V_{measured}$ is the measured voltage at x, x_o an offset from zero, w_o the spot size at that particular location along the optical axis, and plus or minus depending upon the direction the blade is translated, i.e. to occlude the beam, or to reveal the beam. An example fit is pictured below in Figure 4

The spot sizes determined by these fits can be seen below:

After extracting the parameters of these fits, we fit the spot sizes to the equation which describes how beam size propagates along the optical axis, as follows:

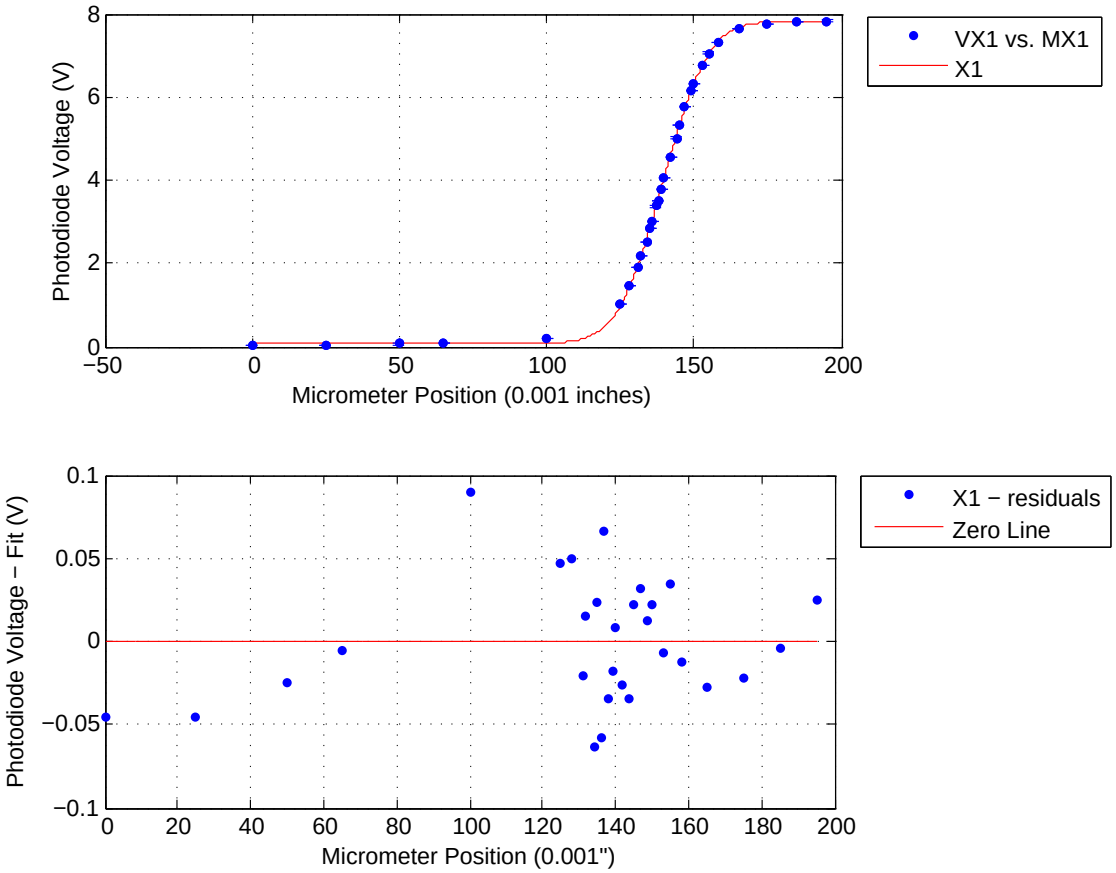

Figure 4: A sample plot of one cross section of the beam

Table 1: Spot Size Measurements

Z Pos. (m)	X Spot Size (μm)	Y Spot Size (μm)
0.0508	615.2 ± 10.67	574.0 ± 13.72
0.0762	272.8 ± 4.83	294.1 ± 10.16
0.1016	50.2 ± 2.64	32.6 ± 3.73
0.1270	293.4 ± 10.67	281.2 ± 9.14
0.1524	637.0 ± 15.49	548.1 ± 16.00
0.1778	926.3 ± 12.70	827.3 ± 17.53

$$w_z = w_o\sqrt{1 + \frac{(z^2\lambda^2}{\pi^2 w_o^2}} \text{ [6]}$$

Where w_z is the beam size at a particular value along the optical axis, w_o is the beam waist, z_r is the rayleigh range of the beam, and b and c are offsets in the w_z and z respectively. (We choose the optical axis to be the Z-Direction.) A sample of this fit is picture in Figure 5

This final fit yields the overall measurement of the beam waist, defined below.

Table 2: Beam Waists After Lens

X Waist (μm)	Y Waist (μm)
907.5 ± 4.5	840.5 ± 3.0

Unfortunately, since the waist of the actual NPRO was outside of the practical range afforded by the optical table the experiment was carried out on, a lens was used (as pictured in Figure 3) to focus the beam, so that we could take measurements near the waist, which affords a much better fit of the spot sizes vs Z Position. Once the waist after the lens can be determined, we can calculate the overall beam waist with the following equation:

$$w_f = \frac{\lambda f}{\pi w_o}$$

Where w_f is the waist after the lens, λ is the wavelength of the laser (1064nm), w_o is the beam waist before the lens, and f is the focal length of the lens ($75mm$) [4].

After this calculation is done, we arrive at the following final beam waists:

Table 3: Beam Waists of Laser

X Waist (μm)	Y Waist (μm)
135.4 ± 214.2	318.1 ± 316.7

Waist Fit.pdf

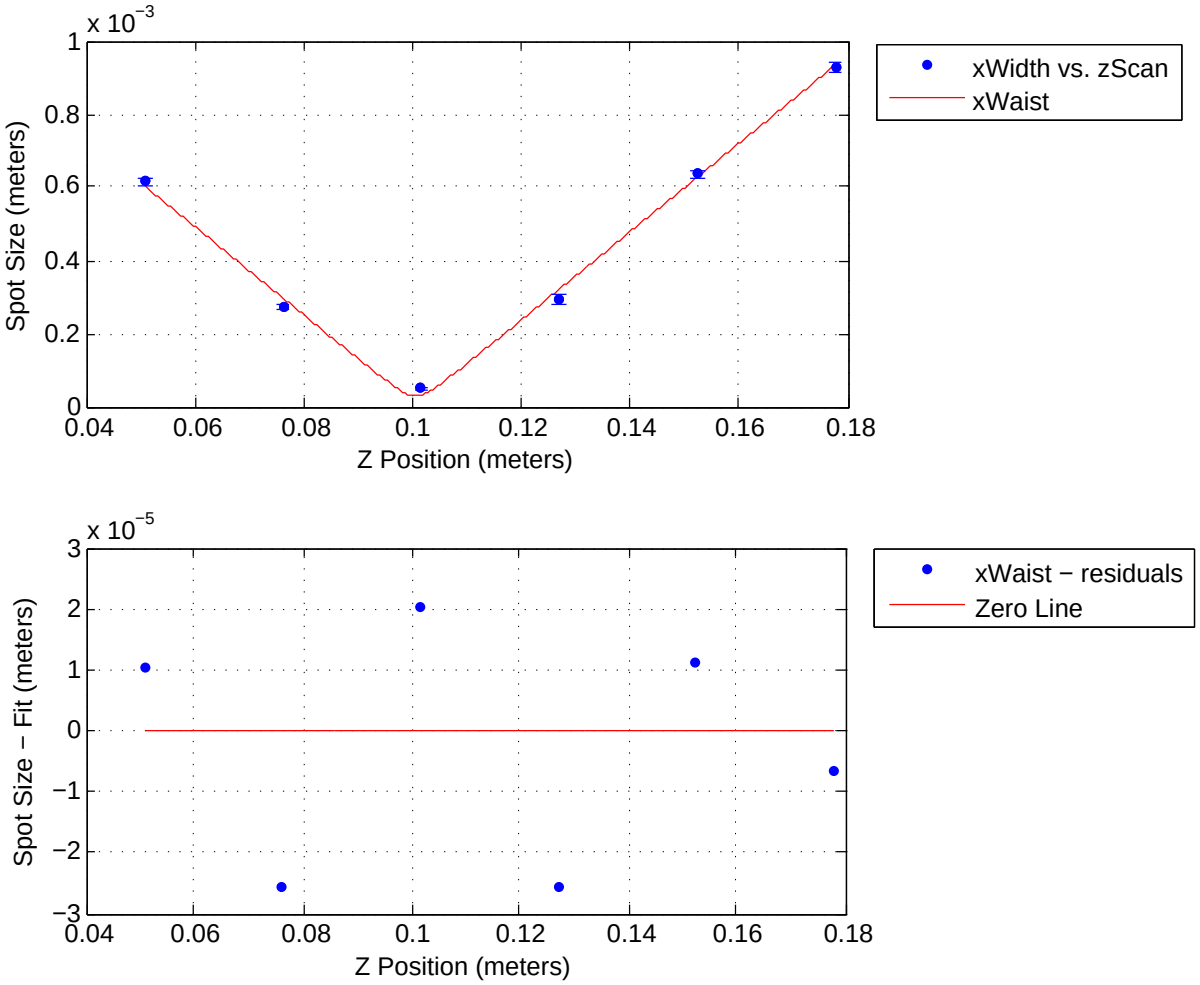

Figure 5: A sample waist measurement plot.

7 Beam Profiler

The second, more modern method to measure a beam waist, is to use a beam profiler. This is an instrument which takes real time, continuous samples of cross sections of the beam, yielding an immediate measurement of spot size. Our beam profiler specifically, is a Thorlabs BP 209-VIS. These spot sizes are then fit to the same equation as those found through the more traditional knife edge measurement, and the waist is extracted as a parameter of this fit.

Using this technique, I was finally able to extract a measurement of 233 μ m, 6cm in front of the NPRO as its waist. This measurement was used successfully in coupling this light to fibers.

8 Telescope Design

In order to couple light to optical fibers, a telescope is employed in order to mode match between the mode intrinsic in the fiber, and that of the NPRO. The NPRO mode has been characterized as described in the section above. It is difficult to characterize fiber modes, until there is light coupled to them. Thus, we use theoretical estimates based upon manufacturers' specifications.

Specifically, our fibers are Corning PANDA PM980 fibers, which have a numerical aperture (NA) of 0.12. This is coupled to a Thorlabs CFC-2X-C collimator, which has a variable lens to fiber distance, and a focal length of 2mm. What we want to calculate is a target waist, which we can use to design a telescope. The NA is determined by the equation below:

$$NA = sin(\theta) \text{ [7]}$$

Given an NA of 0.12, θ is given by the arcsin of the numerical aperture. θ, the collimator focal length, and target waist are related by

$$f = \frac{w}{tan(\theta)} \text{ [8]}$$

We chose the focal length of our collimator to be 2mm. At that point, it is a simple calculation to arrive at a value of 241μm for our target waist. Since the coupling will be performed on an extra optical table, there aren't truly any space constraints, and thus the location of this waist along the optical axis is virtually arbitrary, as the coupling assembly can be placed anywhere.

In order to design this telescope, one uses ABCD matrix analysis. Given the number of possible lens combinations afforded to us, doing this analysis by hand tends to be very tedious and time consuming. Thus, I used A La Mode [9] to parse through all lens combinations possible, given the lens kit available (Thorlabs LSB04-C), and arrived at a system of a single lens, placed 77cm from the NPRO waist. This gives a waist of 231um, located 1.23m from the NPRO waist. It is at this point that I will perform the fiber coupling.

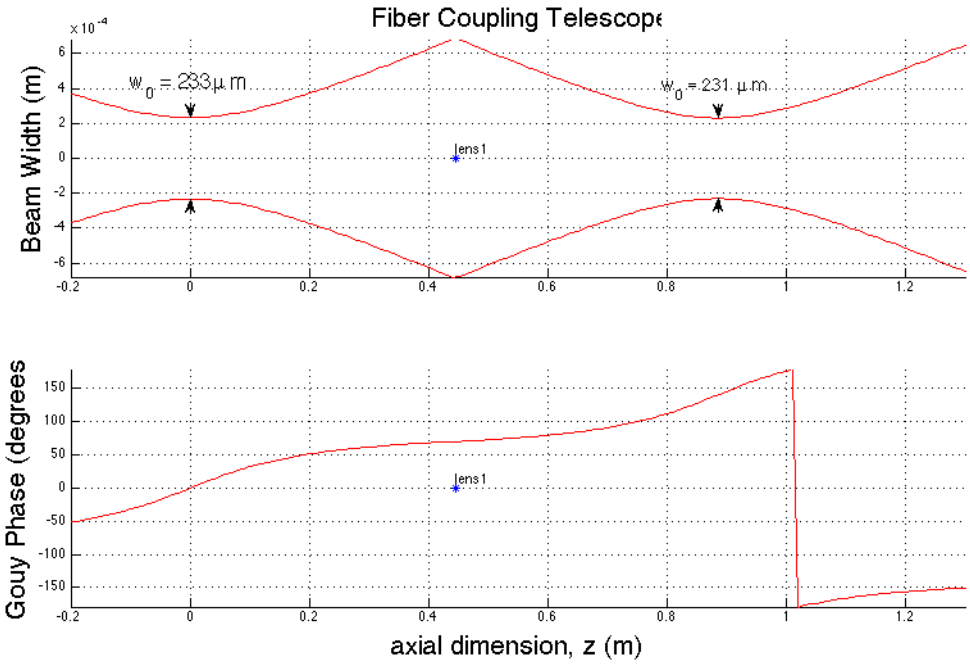

Figure 6: Coupling Telescope Design

9 Fiber Coupling

Fiber coupling laser light is essentially very precise alignment and positioning of the modes of the fiber, and of the laser. Hence the term, mode matching. My setup employed the above described coupling lens, as well as two steering mirrors. The fiber and coupler were held in a 6-axis rotational mount, which allows for tilt, yaw, translation in X and Y, as well as rotation of the fiber about its axis. The rotation is important in order to align the axes of the fibers with the polarization of light.

I found it extremely helpful to first use a fiber illuminator, which sends visible light through the fiber that is subsequently collimated. Qualitatively precise alignment of the illuminated beam, and the NPRO beam can be accomplished in such a manner.

After this was done, the illuminator was traded for a fiber coupled power meter, which read out the optical power coupled into the fiber. Different degrees of freedom were tuned, until the power meter read a maximum value.

In my case, the maximum power I was able to couple was 37mW, which is gives a coupling of 46.25% given the beam power before the fiber is roughly 80mW. Though this was the best coupling I was able to achieve, it typically is around 30%, $\pm$ 5%. This coupling is sufficient for the purposes it will be used for. When coupling is performed on the light from PSL and AUX lasers for use in frequency offset locking, the coupling will be much higher.

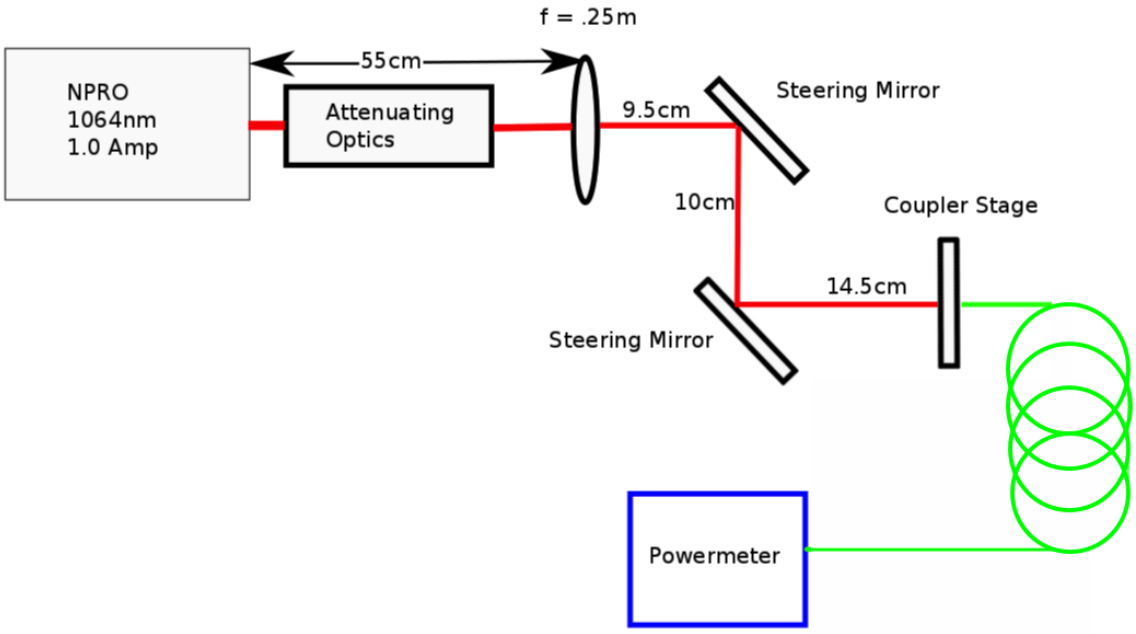

Figure 7: Fiber Coupling Schematic

10 Fiber Testing

Since we will be implementing these polarization maintaining fibers in the frequency offset locking setup, we want to know their characteristics that could effect the function of the system. Nominally, the qualities to be tested are the polarization extinction ratio of the fibers, frequency noise introduced by the fibers, and the effects a temperature gradient along the fiber could have on the output, in terms of noise and polarization. As of yet, we have only been able to start setting up to measure the Polarization Extinction Ratio, which has run into a few problems itself.

11 Polarization Extinction Ratio

The Polarization Extinction Ratio (PER) is defined by a system, where linearly polarized light is injected, and light with some ellipticity is returned. The quantity is described below:

$$PER = 10log_{10}(\frac{P_x}{P_y}) \text{ [10]}$$

Where P_x corresponds to the intensity of the unwanted polarization, and P_y is the intensity of the injected polarization.

This quantity has not yet been measured, as I encountered some problems with the setup, described further in the "Problems" section.

12 Frequency Offset Locking Optical Setup

Essential to the FOL setup is an optical system that will sample the PSL and AUX lasers, and combine them to produce a beat note, which will be used as the error signal in a feedback control loop. The progress thus far in this optical system has been measurement of the beam waists of Y-Arm AUX and PSL light that we will be using to couple into fibers for this system. The pertinent data and figures are pictured below:

13 Methods

13.1 Knife Edge Measurement

Knife Edge measurement of the laser light has proven much more difficult than it seems in principle. For various reasons; too few data points, points too far from the waist of the beam, photodiode saturation, excessively short focal length of the lens, the fits haven't given very accurate results, until the most recent set of measurements. I don't envision other systematic difficulties for this section of the project, as I am now familiar with effective practices for beam waist measurement.

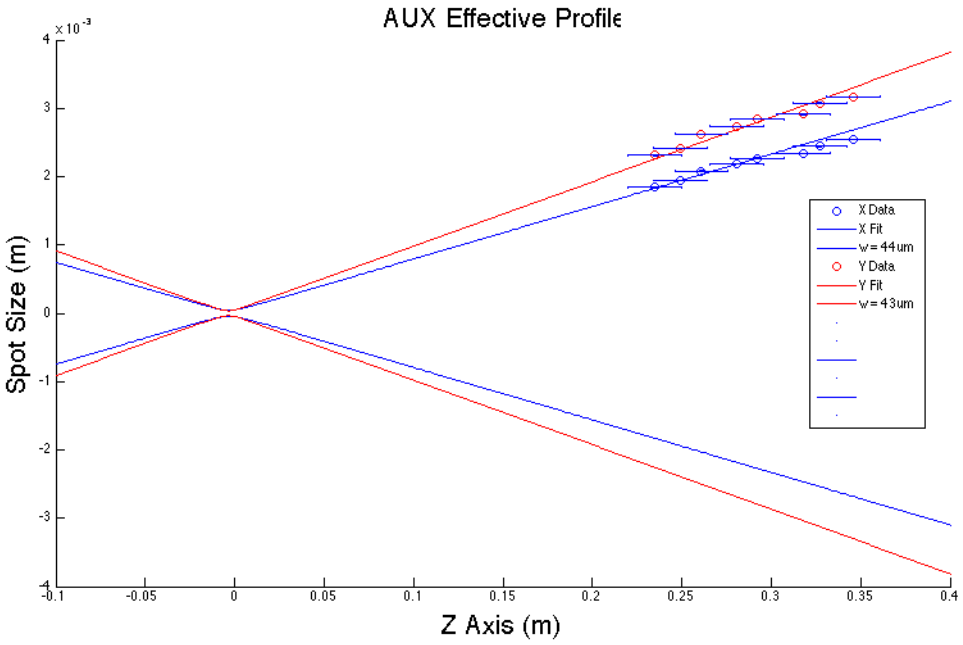

Figure 8: The Y-end laser profile

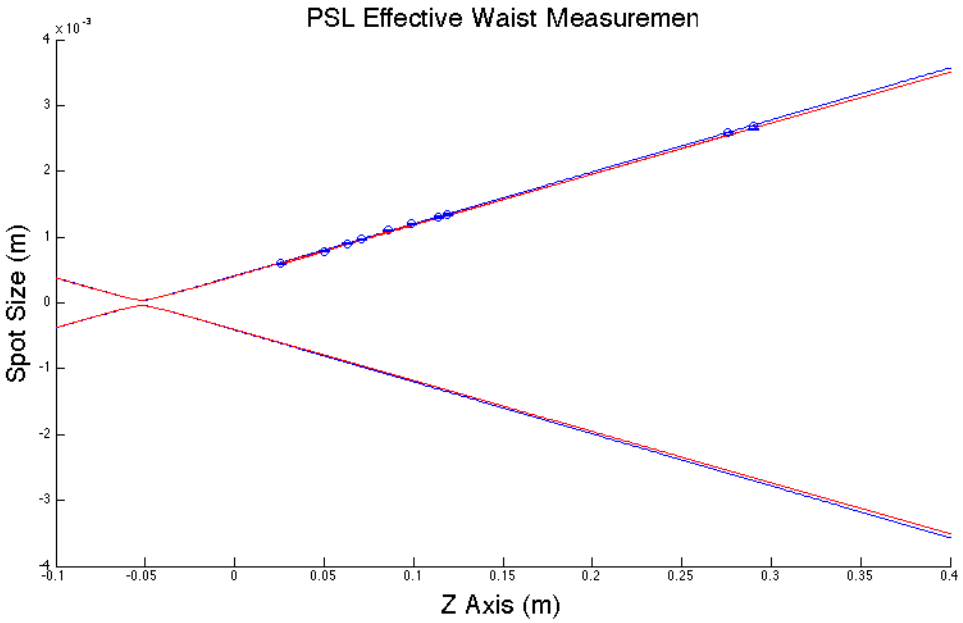

Figure 9: The PSL profile

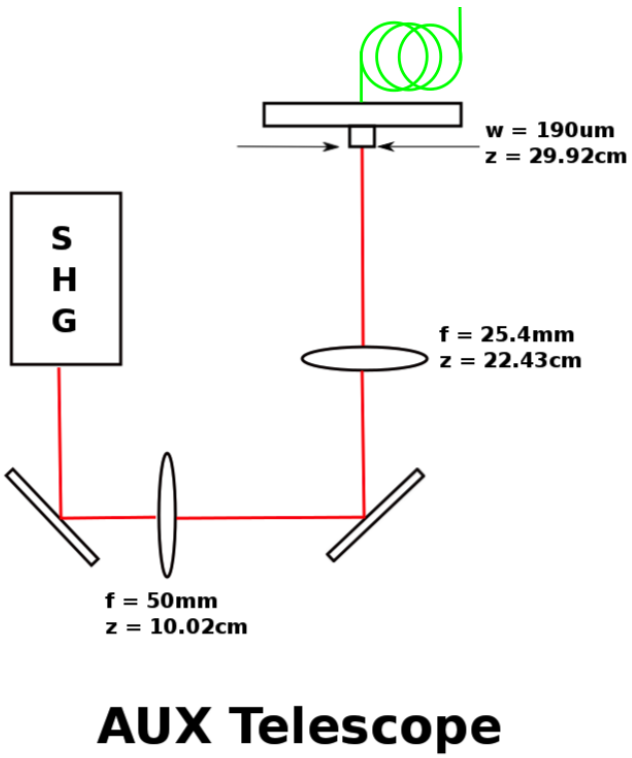

Figure 10: Coupling telescope design for AUX

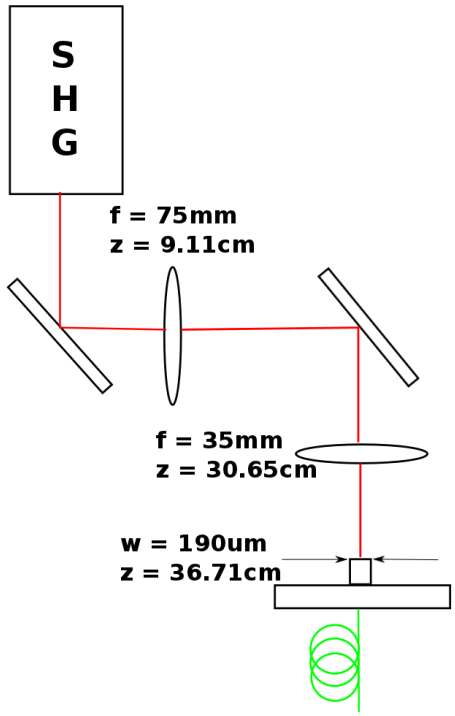

Figure 11: Coupling telescope design for PSL

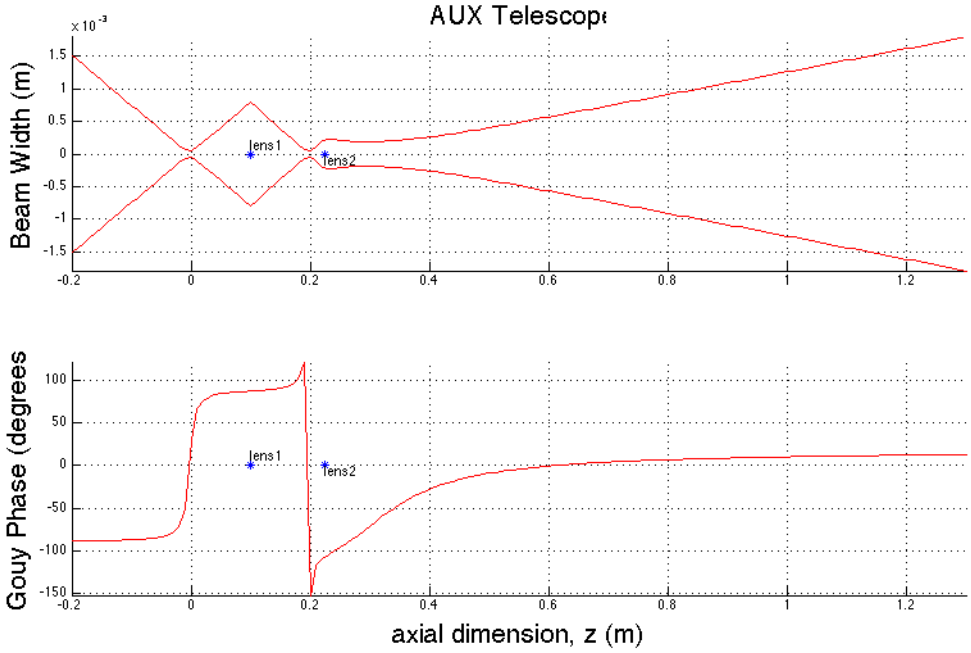

Figure 12: AUX telescope beam profile

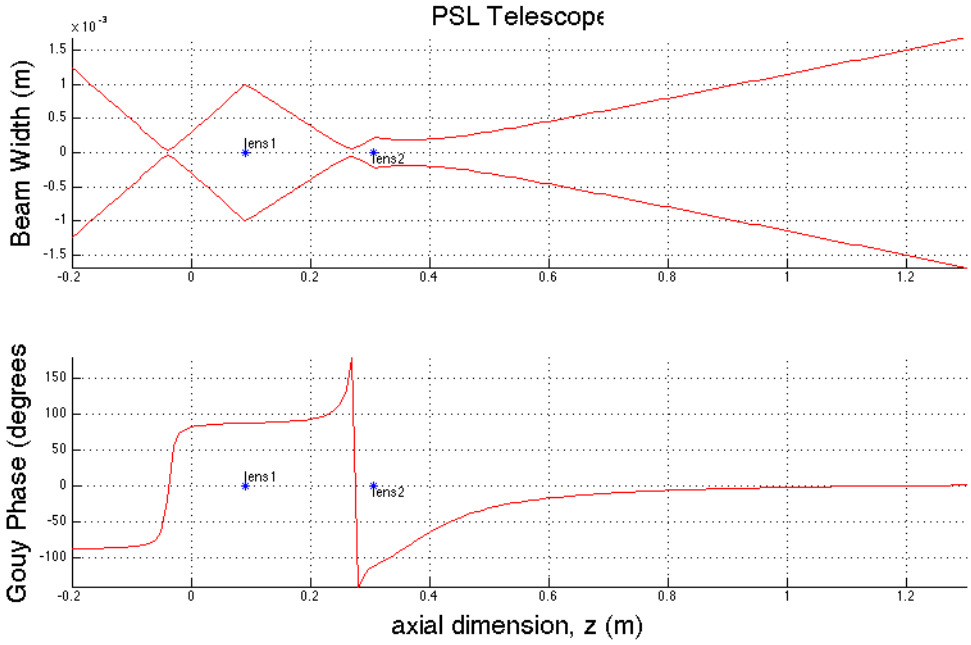

Figure 13: PSL telescope beam profile

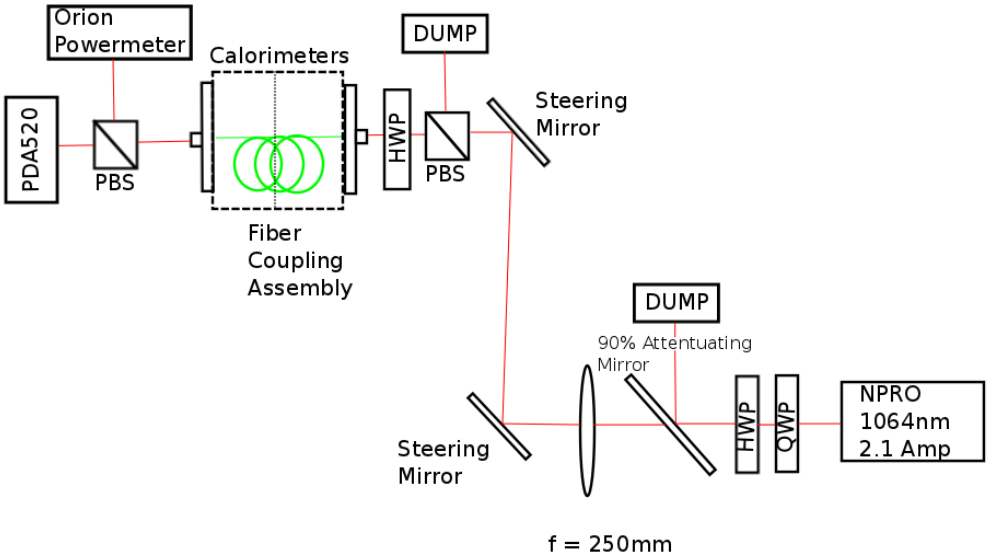

Figure 14: Temperature Affect Measurement

13.2 Polarization Extinction Ratio Setup

In the PER setup, the 6-axis rotational mounts that we use to hold the collimators have too much freedom in their rotational dimension. When the rotation is adjusted to be aligned with the incoming polarization, the torsion from the fibers causes the mount to rotate on its own, making it impossible to take a reliable, consistent measurement of PER. We ordered and have now received new mounts with set screws to lock the rotation in place, and are now waiting on more adapters to connect collimators to the mounts.

13.3 AUX Laser Waist Measurement

In the measurement of the waist of the AUX laser, the location of the measurements within the box made it very difficult to see exactly what the location along the z-axis was. This is what caused such large horizontal error bars in that particular plot. Despite this, in addition to a strangely shaped input beam, the waist locations and sizes seemed to agree with themselves, and should suffice to couple enough light for our purposes.

13.4 Fiber Coupling For FOL

I was only able to fiber couple the Y-Arm AUX laser and PSL with limited success in my initial trials. Around $5mW$ of AUX, and only about $55\mu W$ of PSL. However, these numbers ended up being irrelevant, as I was instructed to stop coupling. My telescope were subsequently dismantled for further use in other experiments, e.g. fiber temperature characterization.

13.5 Fiber Temperature Characterization

The idea behind this was to apply a temperature gradient to the Polarization Maintaining fibers, and observe whether there was any significant effect upon their polarization maintaining qualities. In order to do so, the fiber was coiled into two separate spools, which were each placed inside calorimeters, so their temperatures would be easily controlled and monitored. A thermocouple probe with a digital readout was sealed in each of the calorimeters for monitoring purposes. The detection setup was identical to that of the original PER setup, with the exception of the calorimeters. A heat gun was to be used to raise the temperature of half of the fiber significantly with respect to the other half. As the temperature dropped, meausrements of PER were to be taken. Temperature vs PER plots would then have been made, and trends (if any present) would have been observed. Unfortunately, when I began coupling into the fibers, I found that no light from the fiber illuminator was making it all the way through the fibers. In other words, it broke. I didn't end up with any results from this experiment.

14 Acknowledgements

I would like to acknowledge the LIGO SURF Program for selecting me, the NSF for funding the program, and my mentors, Manasadevi Thirugnasambandam, Eric Quintero, and Koji Arai.

References

[1] http://www.ligo-wa.caltech.edu/ligo_faq.html

[2] Kiwamu Izumi *Multi-Color Interferometry for Lock Acquisition of Laser Interferometric Gravitational-wave Detectors* Department of Astronomy, The University of Tokyo

[3] Masaki Ando *Power recycling for an interferometric gravitational wave detector* Department of Physics, Faculty of Science, niversity of Tokyo

[4] https://marketplace.idexop.com/store/IdexCustom/PartDetails?pvId=24925

[5] http://pendientedemigracion.ucm.es/info/euoptica/org/pagper/jalda/docs/libr/laserandgaussian_eoe_03.pdf

[6] http://www.rp-photonics.com/focal_length.html

[7] http://micro.magnet.fsu.edu/primer/anatomy/numaperture.html

[8] http://www.thorlabs.com/tutorials.cfm?tabID=38696

[9] https://github.com/nicolassmith/alm

[10] http://www.fibercore.com/expertise/fiberpaedia/polarization-extinction-ratio-per